A volume-based hydrodynamic approach to sound wave propagation in a monatomic gas

A volume-based hydrodynamic approach to sound wave propagation in a monatomic gas

S. Kokou Dadzie and Jason M. Reese

Citation: Physics of Fluids (1994-present) **22**, 016103 (2010); doi: 10.1063/1.3292011
View online: http://dx.doi.org/10.1063/1.3292011
View Table of Contents: http://scitation.aip.org/content/aip/journal/pof2/22/1?ver=pdfcov
Published by the AIP Publishing

A volume-based hydrodynamic approach to sound wave propagation in a monatomic gas

S. Kokou Dadzie[a] and Jason M. Reese[b]
Department of Mechanical Engineering, University of Strathclyde, Glasgow G1 1XJ, United Kingdom

(Received 21 March 2009; accepted 14 December 2009; published online 15 January 2010; publisher error corrected 19 January 2010)

We investigate sound wave propagation in a monatomic gas using a volume-based hydrodynamic model. In Dadzie *et al.* [Physica A **387**, 6079 (2008)], a microscopic volume-based kinetic approach was proposed by analyzing molecular spatial distributions; this led to a set of hydrodynamic equations incorporating a mass-density diffusion component. Here we find that these new mass-density diffusive flux and volume terms mean that our hydrodynamic model, uniquely, reproduces sound wave phase speed and damping measurements with excellent agreement over the full range of Knudsen number. In the high Knudsen number (high frequency) regime, our volume-based model predictions agree with the plane standing waves observed in the experiments, which existing kinetic and continuum models have great difficulty in capturing. In that regime, our results indicate that the "sound waves" presumed in the experiments may be better thought of as "mass-density waves," rather than pressure waves. © *2010 American Institute of Physics*.
[doi:10.1063/1.3292011]

I. INTRODUCTION

One of the assumptions underpinning the conventional Navier–Stokes–Fourier set of equations is that of local thermodynamic equilibrium. This assumption allows the representation of thermodynamic variables (e.g., temperature, density, pressure) as locally constant at a given time and position, and the use of equations of state. The assumption that microscopic relaxation processes are not of concern is, however, inadequate in flows where the microscopic relaxation time is comparable to the characteristic time of evolution of the macroscopic field variables. In the kinetic theory of dilute gases, such flows are identified with high Knudsen numbers (conventionally defined as a ratio of the average time between molecule/molecule collisions to a macroscopic characteristic time of the flow, however, see Ref. 1). Experimental observations of sound wave propagation at high Knudsen number challenge many continuum hydrodynamics and kinetic theory models;[2–5] it is well known that the Navier–Stokes–Fourier model fails to predict sound wave propagation at high Knudsen number. Another problem arises in the so-called "heat conduction paradox," according to which an unphysical infinite speed of thermal wave propagation is predicted by the energy equation closed with Fourier's law.

Generally, techniques for investigating gas flows in which the Navier–Stokes–Fourier model is inadequate are based on approximate solutions to the Boltzmann dilute gas kinetic equation, for which a wide number of mathematical methods are found in the literature.[3] Regarding the specific problem of predicting sound wave propagation in monatomic gases in the high Knudsen number regime, many of these Boltzmann based approximations fail, as does Navier–Stokes–Fourier.[3–7] While a few have shown some agreement with experiments,[8,9] detailed analysis makes any conclusion far from clear-cut.[3,10–12] For example, if the experimental setup is configured to measure propagations of plane harmonic waves,[8] Boltzmann kinetic models predict unconventional pressure fields, even though the phase speeds and damping coefficients do agree with the experimental data.[9] Recently developed continuum models also show discrepancies in these predictions, particularly in the damping.[10,13]

The unphysical predictions of the conventional Navier–Stokes–Fourier model have been investigated in terms of the "heat conduction paradox." Early investigations criticized the expression of Fourier's law, suggesting instead that the heat flux expression should be transformed from the parabolic form of the heat conduction equation to a simple hyperbolic equation with a finite speed of propagation. While the original demonstration by Cattaneo[14] has a flaw,[15] a Cattaneo–Vermot heat flux has been formalized more elegantly using fading memory theory (which essentially aims to remove the local equilibrium assumption). Variants and generalizations have been proposed, and compatibility with the second law of thermodynamics has been assessed.[16,17] However, these investigations concentrate on modifications to the simple heat conduction equation; they are not, to our knowledge, developed within the framework of complete fluid dynamic equations and a full dispersion analysis.

In this paper we investigate a continuum model in which the assumptions limiting the application of the conventional Navier–Stokes–Fourier model are clearly released; this is therefore outside the framework of pure approximation solutions to the Boltzmann kinetic equation. In previous work, we proposed releasing the local equilibrium assumption by

[a]Electronic mail: kokou.dadzie@strath.ac.uk.
[b]Electronic mail: jason.reese@strath.ac.uk.

including the spatial distributions of molecules within the kinetic description.[18] While our description was motivated by an unusual volume diffusion claimed by Brenner,[19,20] it has been recently pointed out that the original Brenner modification does not predict sound wave speeds correctly.[21,22]

Here we show that our volume-based hydrodynamic model can reproduce the experimental sound wave propagation data from Ref. 5 with excellent agreement. Moreover, our model offers a more reliable explanation of the experiments, which were designed to range up to the free molecular regime in which there are no collisions between molecules and therefore the definition of sound as a pressure wave becomes problematic.

This paper starts with a summary of our volume model that incorporates effects from microscopic spatial distributions of the gaseous molecules. Subsequently, a linear stability analysis of the model equations is performed, and the predicted dispersion and damping compared with experiments.

II. SUMMARY OF THE VOLUME-BASED HYDRODYNAMIC DESCRIPTION

The traditional single particle distribution function used in the Boltzmann kinetic equation for a monatomic gas attributes no particular importance to the spatial arrangements of molecules. An average number of molecules is associated with a position X and a velocity ξ. In order to account for microscopic spatial fluctuations, due to nonuniformity in molecular spatial configurations, we considered within the set of microscopic variables the microscopic free volume, v, around each gaseous molecule. A single particle distribution function $f(t,X,\xi,v)$ is then defined to describe the probability that a molecule at a given time t is located in the vicinity of position X, has its velocity in the vicinity of ξ, and has around it a microscopic free space given by the additional variable v.

A Boltzmann-like kinetic equation for $f(t,X,\xi,v)$ is then derived as[18]

$$\frac{\partial f}{\partial t}+(\xi\cdot\nabla)f+W\frac{\partial f}{\partial v}=\int\int(f^{+}f_1^{+}-ff_1)\sigma\xi_r d_\omega d_{\xi_1}, \tag{1}$$

in which the term on the right-hand-side is the hard sphere molecule collision integral; $f=f(t,X,\xi,v)$ and $f_1=f(t,X,\xi_1,v_1)$ refer to postcollision molecules, $f^{+}=f(t,X,\xi^{+},v^{+})$ and $f_1^{+}=f(t,X,\xi_1^{+},v_1^{+})$ refer to precollision molecules, $\xi_r=\xi-\xi_1$ is the molecule relative velocity, σ is the collision differential cross section, and d_ω is an element of solid angle. On the left-hand-side appears a new term involving W, which arises primarily from the introduction of the new variable v into the distribution function. In the derivation of Eq. (1), molecular exchanges of momentum through interactions have been assumed to be independent of their spatial configurations.

Three contributions to the time variations of $f(t,X,\xi,v)$ are seen within Eq. (1). Molecular free-stream motions are given by the second term on the left-hand-side. The third term on the left-hand-side arises from effects of molecular interactions on their spatial distributions. Finally, the collision integral is the traditional momentum exchange between molecules that provides changes in molecular velocities. These latter two terms infer that the real molecular potential interactions are represented in this kinetic model by two separate actions: intermolecular force effects on spatial distributions and collisional effects on molecular velocities.

A. Molecular average properties

As $f(t,X,\xi,v)$ is defined as a probability density function, we have a normalization factor,

$$A_n(t,X)=\int_{-\infty}^{+\infty}\int_{0}^{+\infty}f(t,X,\xi,v)d_v d_\xi. \tag{2}$$

The mean value, $\bar{Q}(t,X)$, of a gas property Q is then defined by

$$\bar{Q}(t,X)=\frac{1}{A_n(t,X)}\int_{-\infty}^{+\infty}\int_{0}^{+\infty}Qf(t,X,\xi,v)d_v d_\xi. \tag{3}$$

The local average of v is therefore the local mean free volume $\bar{v}(t,X)$ around each gaseous molecule, i.e.,

$$\bar{v}(t,X)=\frac{1}{A_n(t,X)}\int_{-\infty}^{+\infty}\int_{0}^{+\infty}vf(t,X,\xi,v)d_v d_\xi. \tag{4}$$

From this mean value of the volume around a molecule, we define the mass-density in the vicinity of position X through

$$\bar{\rho}(t,X)=\frac{M}{\bar{v}(t,X)}, \tag{5}$$

where M is the molecular mass. Two mean velocities are defined using two different weighting values: the local mean mass-velocity, $U_m(t,X)$, is given through

$$A_n(t,X)U_m(t,X)=\int\int\xi f(t,X,\xi,v)d_\xi d_v, \tag{6}$$

and a local mean volume-velocity, $U_v(t,X)$, by using the microscopic free volume as the weighting,

$$\bar{v}(t,X)A_n(t,X)U_v(t,X)=\int\int v\xi f(t,X,\xi,v)d_\xi d_v. \tag{7}$$

The two definitions U_v and U_m coincide if v is a constant, i.e., in a homogeneous medium where density is constant throughout. It can be shown that the difference between these two velocities, $U_v-U_m=\bar{v}^{-1}\mathbf{J}_v$, behaves like a mass-density diffusion.[18]

B. A volume-based hydrodynamic set of equations

Hydrodynamic equations are derived as conservation equations obtained from the kinetic equation, accounting for a reclassification of convective/diffusive fluxes required by the appearance of the two different velocities. The set of equations is obtained:[18]

- Continuity,

$$\frac{DA_n}{Dt} = -A_n \nabla \cdot U_m. \tag{8}$$

- Mass-density,

$$A_n \frac{D\bar{v}}{Dt} = -\nabla \cdot [A_n \mathbf{J}_v] + A_n W. \tag{9}$$

- Momentum,

$$A_n \frac{DU_m}{Dt} = -\nabla \cdot A_n \left(\mathbf{P}' - \frac{1}{\bar{v}^2} \mathbf{J}_v \mathbf{J}_v \right). \tag{10}$$

- Energy,

$$A_n \frac{D}{Dt} \left[\frac{1}{2} U_m^2 + e'_{\text{in}} - \frac{1}{2\bar{v}^2} \mathbf{J}_v^2 \right] = -\nabla \cdot A_n \left[\left(\mathbf{P}' - \frac{1}{\bar{v}^2} \mathbf{J}_v \mathbf{J}_v \right) \cdot U_m \right] - \nabla \cdot A_n \left[\mathbf{q}' + \frac{1}{\bar{v}} \mathbf{P}' \cdot \mathbf{J}_v + \frac{1}{\bar{v}} \left(e'_{\text{in}} - \frac{1}{\bar{v}^2} \mathbf{J}_v^2 \right) \mathbf{J}_v \right], \tag{11}$$

where we denote the material derivative $D/Dt \equiv \partial/\partial t + U_m \cdot \nabla$. The flow variables are the probability density A_n (which is, however, not a physical property), the mass-density $\bar{\rho}$, the mass-velocity U_m, and the internal energy e'_{in}.

Following, provisionally, the classical phenomenological Fick's law for a diffusive flux, the model may be closed by the constitutive relations:

$$\frac{M\mathbf{P}'_{ij}}{\bar{v}} = p' \delta_{ij} - \mu' \left(\frac{\partial U_{v_i}}{\partial X_j} + \frac{\partial U_{v_j}}{\partial X_i} \right) + \eta' \frac{\partial U_{v_k}}{\partial X_k} \delta_{ij}, \tag{12}$$

$$\frac{M\mathbf{q}'}{\bar{v}} = -\kappa'_h \nabla T', \tag{13}$$

$$\mathbf{J}_v = -\kappa_m \nabla \bar{v}, \tag{14}$$

in which we defined $Me'_{\text{in}} = (3/2)kT'$ with T' being the kinetic temperature, or $p' = (2/3)\bar{\rho} e'_{\text{in}}$ with p' being the kinetic pressure, and $U_v = U_m + \bar{v}^{-1} \mathbf{J}_v$. The coefficients μ', κ'_h, η', and κ_m are, respectively, dynamic viscosity, heat conductivity, bulk viscosity, and the mass-density diffusion coefficient. As the kinetic pressure p' is defined by the trace of the pressure tensor we also have $(2/3)\mu' - \eta' = 0$.

Previous volume diffusion hydrodynamic models have been based on separating the mean velocity in the conventional mass conservation equation (continuity equation), from the mean velocity in the Navier–Stokes momentum equation via Newton's viscosity law.[20] This has proven controversial[23]—problems in differentiating the mass-flux from the momentum density, and in conserving angular momentum when the velocity on the left-hand-side of the Navier–Stokes equation is substituted for, have been raised. In our approach, however, a mass flux is given by $\bar{\rho} U_v$ from the mass-density Eq. (9), and involves the same velocity, $U_v = U_m + \bar{v}^{-1} \mathbf{J}_v$, as in Newton's viscosity law [Eq. (12)]. Meanwhile, the velocity on the left-hand-side of the new momentum Eq. (10) remains the conventional mass velocity U_m (following Newton's second law). Consequently the two flaws mentioned in connection with volume-based hydrodynamics in Ref. 23 are not present in our set of Eqs. (8)–(14).

C. The localized rate of change of volume, *W*

A consequence of our localized microscopic volume description is the appearance of W, the time rate of change of microscopic volume. Although this term could be proposed using details of the interactions between particles, here we instead test a phenomenological expansion of $W = \delta v / \delta t$ as a function of the fluid macroscopic thermodynamic variables. First we relate variations of the microscopic v to variation of its macroscopic average $\bar{v}$, through a relaxation approximation

$$\frac{\delta v}{\delta t} = \frac{d}{dt} \left(\bar{v} + \tau_s \frac{d\bar{v}}{dt} \right). \tag{15}$$

The derivative $\delta/\delta t$ refers to the time rate of change in microscopic properties while d/dt refers to the time rate of change of macroscopic properties, with τ_s as a relaxation time. Expanding $d\bar{v}$ as a function of thermodynamic variables we have

$$\frac{1}{\bar{v}} W = \alpha \frac{dT'}{dt} + \beta \tau_s \frac{d^2 T'}{dt^2} - \chi \frac{dp'}{dt} - \gamma \tau_s \frac{d^2 p'}{dt^2}, \tag{16}$$

where α, β, χ, and γ are the gas expansion and compressibility coefficients given by

$$\alpha = \left(\frac{1}{\bar{v}} \frac{\partial \bar{v}}{\partial T'} \right)_{p'}, \quad \chi = -\left(\frac{1}{\bar{v}} \frac{\partial \bar{v}}{\partial p'} \right)_{T'}, \tag{17}$$

and

$$\beta = \left(\frac{1}{\bar{v}} \frac{\partial^2 \bar{v}}{\partial T'^2} \right)_{p'}, \quad \gamma = -\left(\frac{1}{\bar{v}} \frac{\partial^2 \bar{v}}{\partial p'^2} \right)_{T'}. \tag{18}$$

In our description local thermodynamic equilibrium is not required. Relations $Me'_{\text{in}} = (3/2)kT'$ and $p' = (2/3)\bar{\rho} e'_{\text{in}}$ define the temperature and pressure (following their classical definitions in kinetic theory), therefore there is a reciprocal relation between temperature and pressure, $p' = kT'/\bar{v}$, by construction without further assumption. If the perfect gas (equilibrium) equation of state is enforced, and we confuse $\delta v/\delta t$ with $d\bar{v}/dt$ in Eq. (16), then the gas expansion and compressibility coefficients in Eq. (17) are the ideal gas coefficients, i.e., $\alpha = 1/T'$ and $\chi = 1/p'$, and the second order contributions vanish from Eq. (16). But as we are not restricting ourselves to local thermodynamic equilibrium, a departure from these ideal coefficients may be expected. Now we turn to investigate sound dispersion using both the first and the second order approximations to W given in Eq. (16).

III. LINEAR STABILITY ANALYSIS AND SOUND WAVE PROPAGATION

A. Linearized one-dimensional equations

We consider our hydrodynamic model in a one-dimensional flow configuration. An equilibrium ground state is defined by the flow variables A_n^0, $\bar{\rho}^0$, T^0, $p^0=R\bar{\rho}^0T^0$, $U_m^0=U_v^0=0$, with R as the specific gas constant. Then a perturbation from this ground state is introduced as follows:

$$A_n = A_n^0(1+A_n^*), \quad \bar{\rho} = \bar{\rho}^0(1+\rho^*), \quad T' = T^0(1+T^*),$$
$$U_m = U_m^*\sqrt{RT^0}, \quad p' = p^0(1+p^*), \tag{19}$$

where the asterisked variables represent dimensionless quantities. The perturbation of the volume velocity is specified through the relationship $U_v=U_m+\bar{v}^{-1}\mathbf{J}_v$. Linearizing $p'=kT'/\bar{v}$ gives $p^*=\rho^*+T^*$. The dimensionless space and time variables are given by

$$x = Lx^*, \quad t = \frac{L}{\sqrt{RT^0}}t^* = \tau t^*, \tag{20}$$

with $\tau=L/\sqrt{RT^0}$. The dimensionless linearized equations, including the general expression for W in Eq. (16), can therefore be written:

- Continuity,

$$\frac{\partial A_n^*}{\partial t^*} + \frac{\partial U_m^*}{\partial x^*} = 0. \tag{21}$$

- Mass-density,

$$(1-\chi^*)\frac{\partial \rho^*}{\partial t^*} - \kappa_m^*\frac{\partial^2\rho^*}{\partial x^{*2}} + (\alpha^*-\chi^*)\frac{\partial T^*}{\partial t^*} - \gamma^*\frac{\partial^2\rho^*}{\partial t^{*2}} + (\beta^*-\gamma^*)\frac{\partial^2 T^*}{\partial t^{*2}} = 0. \tag{22}$$

- Momentum,

$$\frac{\partial U_m^*}{\partial t^*} - \frac{4}{3}\mu^*\frac{\partial^2 U_m^*}{\partial x^{*2}} + \frac{\partial A_n^*}{\partial x^*} + \frac{\partial T^*}{\partial x^*} - \frac{4}{3}\mu^*\kappa_m^*\frac{\partial^3\rho^*}{\partial x^{*3}} = 0. \tag{23}$$

- Energy,

$$\frac{\partial T^*}{\partial t^*} + \frac{2}{3}\frac{\partial U_m^*}{\partial x^*} - \frac{2}{3}\kappa_h^*\frac{\partial^2 T^*}{\partial x^{*2}} + \frac{5}{3}\kappa_m^*\frac{\partial^2\rho^*}{\partial x^{*2}} = 0, \tag{24}$$

where the different dimensionless transport coefficients are given through

$$\mu' = \bar{\rho}^0 L\sqrt{RT^0}\mu^*, \quad \kappa_m = L\sqrt{RT^0}\kappa_m^*,$$
$$\kappa_h' = \frac{L\bar{\rho}^0(\sqrt{RT^0})^3}{T^0}\kappa_h^*, \tag{25}$$

and

$$\alpha = \frac{1}{T^0}\alpha^*, \quad \chi = \frac{1}{p^0}\chi^*, \quad \beta = \frac{1}{T^0}\beta^*,$$
$$\gamma = \frac{1}{p^0}\chi^*, \quad \tau_s = \tau. \tag{26}$$

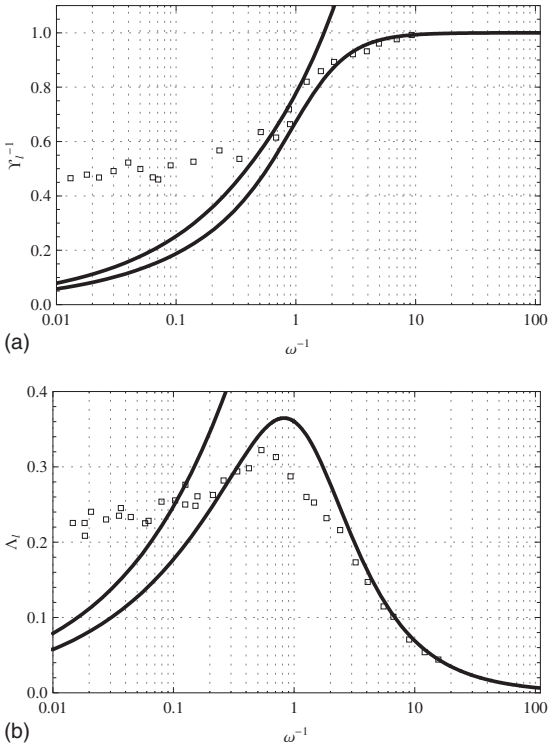

FIG. 1. Comparison of our volume-based dispersion predictions with experiments, with W represented by a first order approximation, and using the definitions in Eq. (32). Experimental data are represented by the discrete squares. With $\alpha^*=\chi^*=1$ the dispersion relation is the same as for the Navier–Stokes–Fourier model. (a) Normalized inverse phase speed varying with ω^{-1}. (b) Normalized damping coefficient varying with ω^{-1}.

Note that the dimensionless transport coefficients in Eqs. (25) follow from the dimensionless form of the hydrodynamic set of equations. Instead of using these dimensionless coefficients, however, it may be more convenient to use conventional parameters, i.e., the Knudsen number K_n, the Prandtl number P_r, and an additional parameter S_c that involves the mass-density diffusivity. These are given by (denoting $\mu^0=\bar{\rho}^0L\sqrt{RT^0}$)

$$K_n = \frac{\mu'\sqrt{RT^0}}{p^0L} \equiv \mu^*, \quad \frac{1}{S_c} = \frac{\kappa_m\bar{\rho}^0}{\mu^0} \equiv \kappa_m^*,$$
$$\frac{1}{P_r} = \frac{2}{5}\frac{\kappa_h'}{R\mu^0} \equiv \frac{2}{5}\kappa_h^*. \tag{27}$$

We assume the disturbances A_n^*, ρ^*, T^*, and U_m^* to be wave functions of the form

$$\phi^* = \phi_a^*\exp[i(\omega t^* - Kx^*)], \tag{28}$$

where ω is the complex wave frequency, K is the complex wave number, and ϕ_a^* is the complex amplitude, so that

$$\frac{\partial \phi^*}{\partial t^*} = i\omega\phi^*, \quad \frac{\partial^2 \phi^*}{\partial t^{*2}} = -\omega^2\phi^*, \quad \frac{\partial \phi^*}{\partial x^*} = -iK\phi^*,$$

$$\frac{\partial^2 \phi^*}{\partial x^{*2}} = -K^2\phi^*, \quad \frac{\partial^3 \phi^*}{\partial x^{*3}} = iK^3\phi^*.$$

The linearized hydrodynamic set of equations then yields the homogeneous system,

$$\Xi(\omega,K) \times \begin{Bmatrix} A_n^* \\ \rho^* \\ T^* \\ U_m^* \end{Bmatrix} = 0, \tag{29}$$

where

$$\Xi(\omega,K) = \begin{Bmatrix} i\omega & 0 & 0 & -iK \\ 0 & \kappa_m^* K^2 + i\omega(1-\chi^*) - \gamma^*\omega^2 & i\omega(\alpha^*-\chi^*) + (\beta^*-\gamma^*)\omega^2 & 0 \\ 0 & -\frac{5}{3}K^2\kappa_m^* & \frac{2}{3}\kappa_h^* K^2 + i\omega & -\frac{2}{3}iK \\ -iK & -\frac{4}{3}iK^3\mu^*\kappa_m^* & -iK & \frac{4}{3}\mu^* K^2 + i\omega \end{Bmatrix}. \tag{30}$$

The corresponding dispersion relation, obtained when the determinant of $\Xi(\omega,K)$ is zero, is

$$\left[\frac{20i\omega K_n K^4}{9P_r} + \frac{5K^4}{3P_r} + \frac{5}{3}i\omega K^2 - \frac{4}{3}\omega^2 K_n K^2 - \frac{5\omega^2 K^2}{3P_r} - i\omega^3\right] \times \left[-\gamma^*\omega^2 + i(1-\chi^*)\omega + \frac{K^2}{S_c}\right] - \left[(\beta^*-\gamma^*)\omega^2 + i(\alpha^*-\chi^*)\omega\right] \times \left[-\frac{4i\omega K_n K^4}{3S_c} - \frac{5K^4}{3S_c} + \frac{5\omega^2 K^2}{3S_c}\right] = 0. \tag{31}$$

B. Dispersion and damping predictions compared with experiment

When analyzing the dispersion and stability characteristics of our model, we compare our results for sound propagation in argon gas, $P_r = 2/3$, with experimental data from Ref. 5. Choosing the harmonic wave expression (28) is in line with previous analysis of this problem, and the dimensionless phase speed Υ_l and dimensionless spatial damping Λ_l are then commonly defined by[4,5,10]

$$\frac{1}{\Upsilon_l} = \sqrt{\frac{5}{3}}\frac{\mathrm{Re}[K]}{\omega}, \quad \Lambda_l = -\sqrt{\frac{5}{3}}\frac{\mathrm{Im}[K]}{\omega}. \tag{32}$$

Setting the Knudsen number K_n, defined in Eq. (27), to 1 makes our analysis agree with that of Greenspan,[4] in which variations of frequency ω are interpreted as variations of Knudsen number (the limitations of this particular interpretation are outlined in the Appendix to this present paper). Although more recent experimental data with a different analysis exist, we choose this approach first in order to make comparisons with previously published works.[4,5,7,10]

We also note here that a solution to a dispersion relation such as Eq. (31) consists of various discontinuous solutions generating a number of modes; one of these is expected to correspond to the sound mode. In this paper, we include in our results figures all modes, for the sake of a complete analysis.

Linear stability criteria are as follows.[22] For the set of equations to be time stable, $\omega(K)$ as a root of the dispersion relation (31) should satisfy $\mathrm{Im}[\omega(K)] \geq 0$ for all K real. On the other hand, the set of equations will be stable in space if $K(\omega)$ as a root of the dispersion relation satisfies $\mathrm{Im}[K(\omega)] \times \mathrm{Re}[K(\omega)] < 0$ for all $\omega \geq 0$.

1. A first order approximation to W: $\beta^* = \gamma^* = 0$

First we set $\beta^* = \gamma^* = 0$, that is, W is approximated only by the first order terms in Eq. (16). For $\alpha^* = \chi^* = 1$ the dispersion and stability characteristics of our model correspond to those of the Navier–Stokes–Fourier model. The equations are also stable in both time and space. Figure 1 shows both the inverse phase speed and the damping as a function of inverse frequency (i.e., inverse Knudsen number), compared with experimental data.[5] Navier–Stokes–Fourier has only two modes: one mode fits the phase speed and damping measurements at low Knudsen number, but has an infinite speed of propagation for high Knudsen number. The second mode shows an infinite inverse phase speed at low Knudsen number and is interpreted as the heat mode.[5,9]

Departures from these predictions are expected for our volume-based hydrodynamic model when $\chi^* \neq \alpha^*$. We find that the model is stable, in the case of a first order approximation to W, if α^* and χ^* are both simultaneously smaller than one, or $\alpha^* \geq 1$ and $\chi^* \leq 0.5$, approximately; this is illustrated in Fig. 2. Comparison of the dispersion with experiments shows globally the same results as in the Navier–Stokes–Fourier case. But, as seen in Fig. 3 where we have $\alpha^* = 0.28$, $\chi^* = 0.48$, and $S_c = 0.9$, the agreement with the low frequency regime is improved, particularly in the damping coefficient. Both the phase speed and the damping are ad-

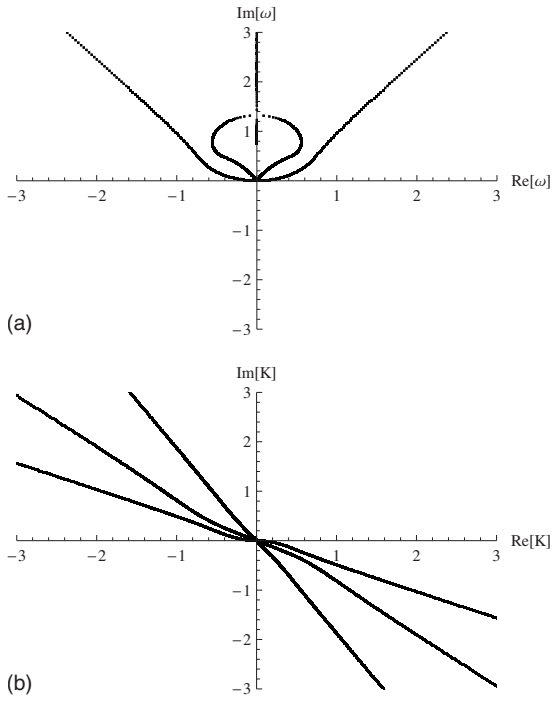

FIG. 2. Stability analysis of our volume-based hydrodynamic equations, with W described by a first order approximation only. Our equations are stable in both space and time if $(\alpha^* \leq 1, \chi^* \leq 1)$ or $(\alpha^* \geq 1, \chi^* \leq 0.5)$. (a) Temporal stability: $\alpha^*=0.28$, $\chi^*=0.48$, $S_c=0.9$. (b) Spatial stability: $\alpha^*=0.28$, $\chi^*=0.48$, $S_c=0.9$.

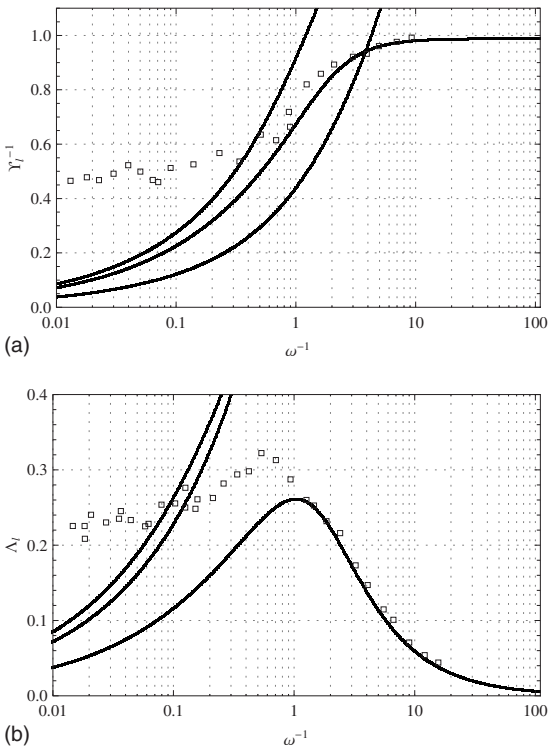

FIG. 3. Comparisons of our volume-based dispersion predictions with experiments, with W represented by a first order approximation, and using the definitions in Eq. (32). Experimental data are represented by the discrete squares. Note the improvement on damping predictions compared to Fig. 1. (a) Normalized inverse phase speed varying with ω^{-1}: $\alpha^*=0.28$, $\chi^*=0.48$, $S_c=0.9$. (b) Normalized damping coefficient varying with ω^{-1}: $\alpha^*=0.28$, $\chi^*=0.48$, $S_c=0.9$.

equately predicted up to $K_n=1$, whereas the damping was predicted only up to $K_n=0.3$ by Navier–Stokes–Fourier alone [Fig. 1(b)].

Figure 3 also shows that there are now three modes, two of which display transient diffusion behavior (i.e., high damping in low frequency regimes). While one of these should be considered as the heat mode, as previously, the other should be attributed to transient mass-density diffusion, as introduced by our new volume-based description (in addition to the heat diffusion). This new mode is the most affected by the mass-density diffusivity, i.e., by S_c. The high frequency regime is still incorrectly predicted by the sound mode, as in the case of Navier–Stokes–Fourier. Later we will see that the infinite speed of propagation and zero damping in the high frequency regime can all be removed with the inclusion of the new mass-density mode.

2. A second order approximation to W, $\alpha^*=\chi^*=0$

Now we set $\alpha^*=\chi^*=0$, that is, W is given by an expression with only the second order terms of Eq. (16). In this case, we observe that the set of volume-based equations has a wider range of stability, provided $0 \leq \gamma^* - \beta^* \leq 1.3$ approximately (see Fig. 4). Figure 5 shows that the phase speed prediction of one of the modes now agrees perfectly with experiment, in both the low and the high frequency regimes. This mode actually corresponds to the pressure mode, and it merges into the new mass-density mode in the high frequency regime. For comparison, in Fig. 6 this physical mode is plotted with the experimental data and results from two recent continuum models derived as approximation solutions to the Boltzmann equation.[10,13] We observe that our volume model is competitive with the best of these two models. Our new model has the best damping coefficient predictions in the low Knudsen number regime, and we note an unphysical negative damping coefficient predicted by the second order model of Spiegel and Thiffeault.[13]

In our investigations, our choice of the values of different coefficients in the volume model has been primarily motivated by finding the best agreement with the experimental data. However, coefficient S_c, set to 0.9 for Fig. 3, agrees with an interpretation of S_c as a Schmidt number with a value of 5/6 for monatomic hard sphere molecular gases; a value of 0.75 has been used for the dispersion analysis in Ref. 21. While the stability depends on the expression of W, our volume-based set of equations seems to remain stable for whatever value the Schmidt number is set to, i.e., whatever the mass-density diffusivity.

The dimensionless expansion and compressibility coefficients we obtained depart from their (equilibrium state) ideal gas values of 1. These departures from ideality may be attributable to real gas effects now incorporated in our volume-based description. Similar results to those presented in our figures are also obtained with other combinations of the various coefficients. For example, $\alpha^*=0.3$, $\chi^*=0.7$, and $S_c=3.33$ give the same results as in Fig. 3. This recalls experimental reports that different gases can produce similar

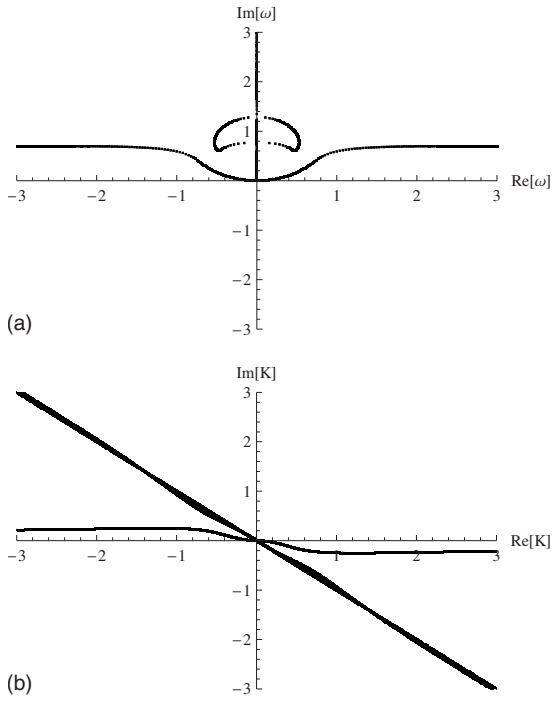

FIG. 4. Stability analysis of our volume-based hydrodynamic equations, with W described by a second order approximation only. Our equations are stable in both space and time if $0 \leq \gamma^* - \beta^* \leq 1.3$. (a) Temporal stability: $\beta^*=0.28$, $\gamma^*=0.48$, $S_c=0.14$. (b) Spatial stability: $\beta^*=0.28$, $\gamma^*=0.48$, $S_c=0.14$.

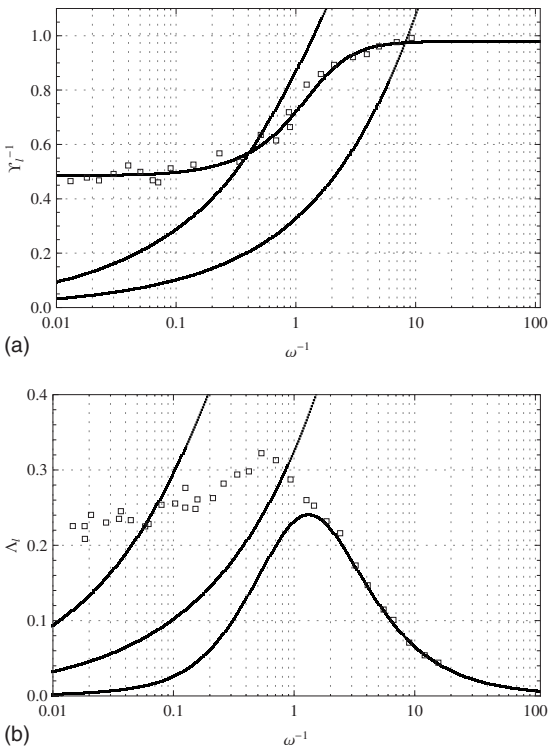

FIG. 5. Comparison of our volume-based dispersion predictions with experiments, with W described by a second order approximation, and using Eq. (32). Experimental data are represented by the discrete squares. Note the agreement with the phase speed for all Knudsen numbers. (a) Normalized inverse phase speed varying with ω^{-1}: $\beta^*=0.28$, $\gamma^*=0.48$, $S_c=0.14$. (b) Normalized damping coefficient varying with ω^{-1}: $\beta^*=0.28$, $\gamma^*=0.48$, $S_c=0.14$.

results.[4,5] In any case, the various coefficients in our volume model leave room to incorporate the various properties of the gas under investigation.

C. A prediction of the damping coefficient in the high frequency regime

In Figs. 1(b), 3(b), and 5(b), the predicted damping coefficient tends to zero as the Knudsen number becomes large. This is a very common result when using continuum models, as seen on Fig. 6. Problems have also been pointed out in comparisons with experiments in this regime.[2,3] Therefore, researchers argued on the basis of spectral analysis that continuum models based on a finite set of partial differential equations cannot capture this branch of the graph.[10] In any case, interpreting sound waves in terms of pressure waves and momentum exchanges between (only) molecules during collisions should be expected to lead to vanishing damping as intermolecular collisions are no longer the dominant phenomena in the very high Knudsen number regime.[6,8]

We now consider earlier comments by some investigators[8,24] who, analyzing the experimental setup, suggested that a model to predict this sound dispersion must have a Knudsen number expression and a dimensional analysis that reflects the distinction between the molecule/molecule collision-dominated regime and the molecule/surface collision-dominated regime.

In the experimental setup the gas was placed between source and receiver then disturbed by a plane harmonic sound wave with a fixed frequency at the source.[5,8,25] The primary variable parameter in the experiments was the distance between the source and the receiver. At very low pressures, the molecule/molecule collisions that predominate in a high pressure (or equilibrium) regime, become negligible, and molecular collisions with surfaces dominate. In this situation, the microscopic collision length scale becomes the distance traveled by molecules to reach the surfaces—no longer the mean free path that is the length scale in the equilibrium regime. Accordingly, Schotter,[8] who also reported similar data to Greenspan, Meyer and Sessler, presents a different dimensional analysis, introducing two different microscopic times leading to two different Knudsen number expressions. The first of these corresponds to a pressure-based intermolecular collision time, and is the same definition as in Refs. 4 and 5. The second microscopic time is independent of molecule/molecule momentum transfers and instead characterizes the frequency of collisions with the surfaces. As we show explicitly in the Appendix, Greenspan's dimensionless quantities in Eq. (32), and the accompanying interpretation of frequency as a (conventional) Knudsen number, are founded on molecule/molecule collisions and so become inappropriate at high Knudsen number where these types of collisions are no longer the principal momentum transfer mechanism (see also Ref. 24). A dimensional analysis using the separation distance between the surfaces leads to a different expression for the dimensional damping coefficient in a low pressure gas, which is also, conversely, invalid for high

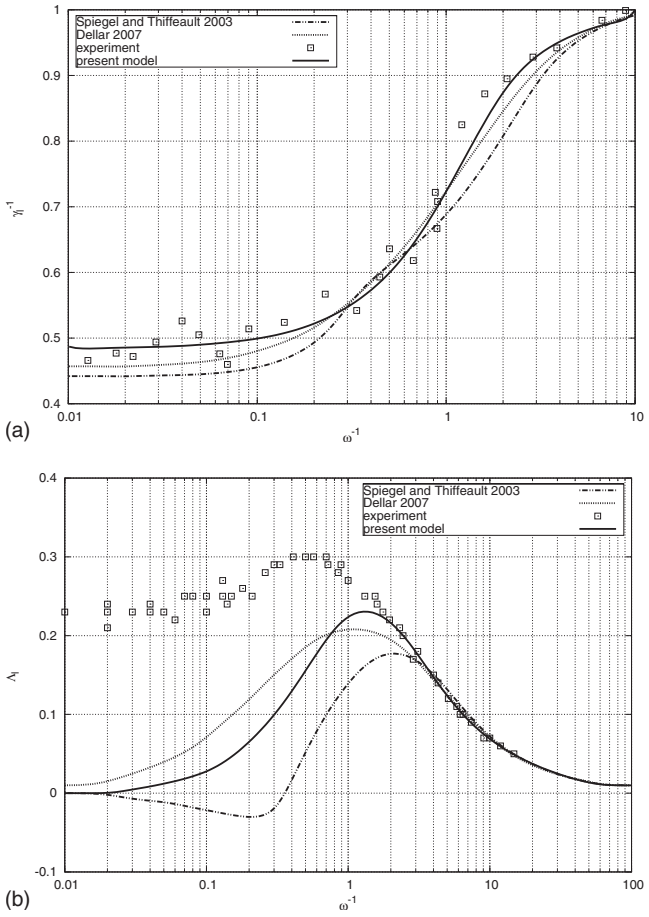

FIG. 6. Comparison of our volume based-model (as in Fig. 5) with two other recent models (Refs. 10 and 13) and argon gas experimental data (Ref. 5). (a) Inverse phase speed compared with other models. (b) Damping coefficient compared with other models.

pressure cases (i.e., at low conventional Knudsen number). This second expression may also be derived using the following observation.

In Sec. III A we performed a dimensional analysis, and introduced Eq. (28) which assumes the harmonic wave form. As the set of partial differential equations is linearized and dimensionless, characteristic time and length scales have therefore been introduced before Eq. (28). A better way of expressing the harmonic wave is in a completely dimensionless form, i.e.,

$$\phi^* = \phi_a^* \exp[i(\omega^* t^* - K^* x^*)], \tag{33}$$

where ω^* and K^* are, respectively, the dimensionless complex wave frequency and dimensionless wave number. Moreover, $\omega^* = \omega\tau$ and $K^* = LK$, with τ and L as the characteristic time and length previously introduced in Eq. (20). The constant coefficient $\sqrt{5/3}$, from the adiabatic exponent of a monatomic gas, could be simply incorporated in the definition of the reference speed and is not here the main issue. The dimensionless phase speed and dimensionless spatial damping coefficient are therefore

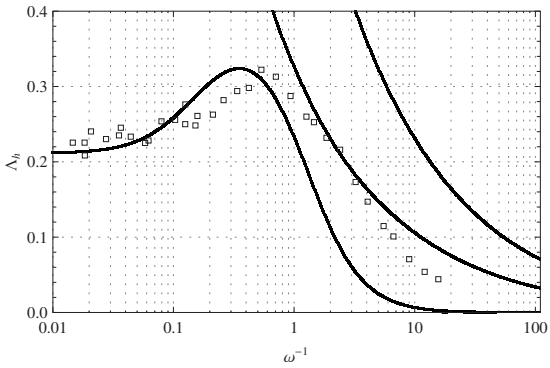

FIG. 7. Damping coefficient predictions with W described by a second order approximation, and using the definitions in Eq. (34); $\beta^* = 0.28$, $\gamma^* = 0.48$, and $S_c = 0.14$. Note the agreement with one of the modes at high Knudsen numbers.

$$\frac{1}{\Upsilon_h} = \sqrt{\frac{5}{3}}\frac{\mathrm{Re}[K^*]}{\omega^*}, \quad \Lambda_h = -\sqrt{\frac{5}{3}}\mathrm{Im}[K^*], \tag{34}$$

and we observe that while the dimensionless phase speed remains the same as previously, the dimensionless damping coefficient is different [see Eq. (32)]: it does not contain the frequency.

In Fig. 7 we plot the dimensionless damping coefficient by our new hydrodynamic model, but using the redefined expressions in Eq. (34) (and using the same coefficients S_c, β^*, and γ^* as in Fig. 5). It is seen that our model reproduces the high frequency branch, with the correct asymptotic value of the damping. In addition, this is represented by the new mass-density mode, not the classical pressure mode which instead diverges. Broadly, this curve catches the shape and the shallow maximum around $K_n \approx 1$. The agreement is not so good by $K_n = 1$ and becomes somewhat inaccurate for low Knudsen numbers, as expected.

In summary, expressions (32) and (34) are each compatible with different Knudsen number regimes and are both required for a proper interpretation of the experimental results. Our volume-based hydrodynamic model has been shown, therefore, to predict both the low and the high frequency branch of the damping coefficient well, while the inverse phase speed is always well predicted.

In his experiments, Schotter[8] reported plane standing waves for all Knudsen numbers. Because of difficulties surrounding the predictions of the high Knudsen number branch, other researchers assumed, however, that a plane wave analysis could not capture this regime.[2,6,10] In our analysis, mass-density and pressure fields are plane harmonic and therefore agree also with Schotter's experimental observation. We also confirm the unusual (i.e., non-pressure-wave) characteristics of sound waves in this regime because our good predictions here are provided by our model's mass-density diffusion terms. This is illustrated in Fig. 8, where the two different modes fitting the experimental damping data in the low and the high frequency regimes are both plotted.

Finally, even with the modified definitions of Eq. (34), the Navier–Stokes–Fourier model gives at $1/K_n = 0.01$ a

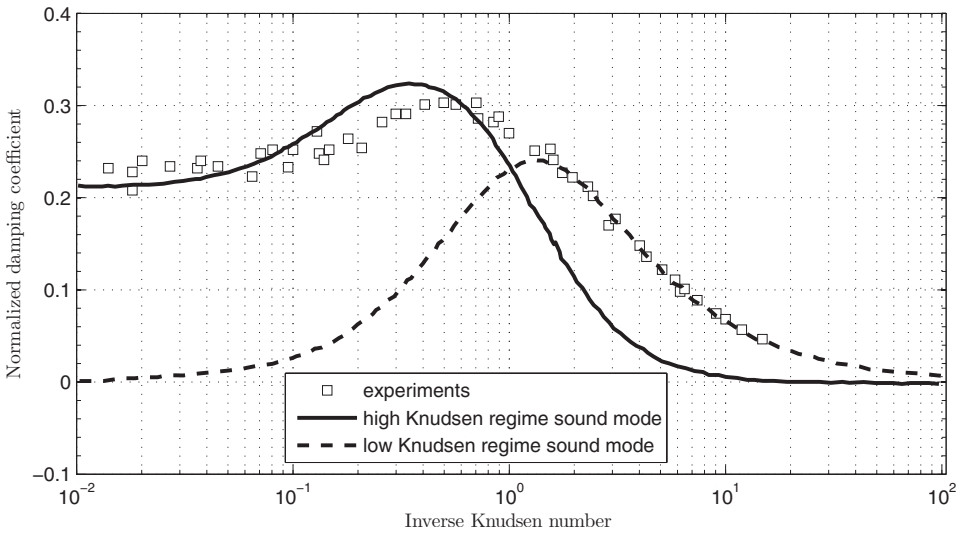

FIG. 8. The two different natures of the sound mode, illustrated by the two different modes fitting experimental damping in different Knudsen number regimes.

value of the damping which is 30 times the experimental value of approximately 0.2. So the conventional model still provides incorrect predictions.

IV. DISCUSSION

Predicting sound wave phase speed and damping is a challenge both for kinetic models derived from the Boltzmann dilute gas equation and for continuum fluid hydrodynamics.[3] The few kinetic models[6,9,11] that agree with the experimental data over the entire range of Knudsen number suffer three major criticisms. First, questions often arise about the compatibility of kinetic boundary value problems with experimental measurement.[2,3] Second, the kinetic models predict nonstandard pressure fields;[9] in contrast, experiments have been based on harmonic pressure waves, and indicate a plane standing wave existing in the gas medium at all Knudsen numbers during measurement. Third, the different mechanisms of momentum transfer in the high pressure and the low pressure cases are not always compatible with the kinetic model predictions.[3,9,24] A final issue, often raised with continuum fluid models beyond Navier–Stokes–Fourier, is the appearance of a large number of modes so it is not always easy to identify the mode that should describe the sound wave.

Our Figs. 5 and 7 show that the continuum-based model considered in this paper reproduces the experiments over the range of Knudsen number without the difficulties listed above. In these figures there are only three distinct modes to be associated with pressure, temperature, and mass-density in a given regime. In our understanding, pressure and mass-density disturbances are distinct plane harmonic waves that dominate in different Knudsen number regimes (see Fig. 8). The existence of a mass-density wave explains the plane standing wave observed in experiments in the high Knudsen number regime; this mode is nonexistent in conventional fluid dynamic equations as there is no explicit mass-density diffusion (or mass-density wave propagation). The agreement between our theoretical damping results and experiment can be fully explained in terms of two mean-free-paths inherent in the experimental setup; one mean free path is founded on the standard kinetic pressure and molecular collisions, and the other is founded on the separation distances of the solid surfaces. The latter also underlines the fundamental basis of our new approach itself: the variation of the surface position is easily associated with variation of the volume between molecules.

Our prediction of the high Knudsen number regime is possible only if we adopt the second-order expression for W given in Eq. (16). This shows that this regime is best described by microscopic structure evolutions and not macroscopic average thermodynamic property evolutions; therefore there is no localized thermodynamic equilibrium in this case. Indeed, in Eq. (15) the time rate of change of the microscopic volume v is represented by the sum of the time rate of change of the average value $\bar{v}$ and the change in its random component, which is approximated using a relaxation time. Consequently, the second-order terms involved in Eq. (16) can be considered expressions of the random component of the microscopic volume evolutions. [A representation of microscopic structure, as in Eq. (15), is common in "fading memory" concepts, where it is given generally as a convolution function.][15,16]

V. CONCLUSION

Our proposed volume-modified hydrodynamic model produces excellent predictions of sound wave dispersion in monatomic gases. Its results also indicate that, in order to properly interpret the experimental data, the difference in the physical mechanisms of "sound wave" propagation at high and low Knudsen numbers needs to be appreciated. This interpretative problem is also, we argue, one of the reasons why previous continuum-fluid models have had such difficulty in capturing sound wave propagation over the whole Knudsen number range.

Our volume representation was originally introduced to allow for spatial microscopic density fluctuations, and in this area there remains scope for its improvement. In particular, a better-validated description of the time rate of change of microscopic volume (W, in the description above) is required as the results presented in this paper suggest some sensitivities

to the expression used. Also the model should be validated against additional benchmark cases, for example, heat transfer in the transition-continuum regime (where the dependency of heat conductivity on the Knudsen number or pressure, and the definition of heat flux are still unresolved problems).[26]

ACKNOWLEDGMENTS

This work is funded in the U.K. by the Engineering and Physical Sciences Research Council under Grant No. EP/D007488/1 and through a Royal Society of Edinburgh/Scottish Government Support Research Fellowship for J.M.R. The authors would like to thank the referees of this paper for their helpful comments.

APPENDIX: ANALYSIS OF GREENSPAN'S INTERPRETATION OF KNUDSEN NUMBER VARIATIONS

This is a boundary value problem, with ω positive real, and $K=(K_r+iK_i)$ a complex number. A plane harmonic wave $\phi(t,x)$ is written with dimensional variables as

$$\phi(t,x)=\exp[i(\omega t-(K_r+iK_i)x)]. \tag{A1}$$

We seek dimensionless expressions for the phase speed and damping. First, Eq. (A1) is rewritten,

$$\phi(t,x)=\exp\left[i\omega\left(t-\frac{K_r}{\omega}x\right)\right]\exp\left[\left(\frac{K_i}{\omega}\right)\omega x\right]. \tag{A2}$$

The experimental setup infers a fixed frequency, ω_e.[4,5,8] Suppose that the gas has well-defined microscopic time and length scales, τ and L, respectively, which therefore specify a microscopic speed C_0. We may then define dimensionless frequency, time, and length as

$$\omega=\omega_e\omega^*,\quad t=\tau t^*=\frac{L}{C_0}t^*,\quad x=Lx^*. \tag{A3}$$

Using these definitions, Eq. (A2) becomes

$$\phi(t,x)=\exp\left[i\omega^*\omega_e\tau\left(t^*-\frac{K_r}{\omega}C_0x^*\right)\right]\times\exp\left[C_0\frac{K_i}{\omega}\omega^*\omega_e\tau x^*\right]. \tag{A4}$$

Away from any gas/surface interaction, the mean free time describing the average collision time between two molecules is well defined. We may therefore choose τ to be the time between successive molecular collisions. In such a case, and with ω_e defining the flow macroscopic time scale, we have a Knudsen number $K_n=\omega_e\tau$. Subsequently, Eq. (A4) yields

$$\phi(t,x)=\exp\left[i\omega^*K_n\left(t^*-\frac{K_r}{\omega}C_0x^*\right)\right]\times\exp\left[C_0\frac{K_i}{\omega}\omega^*K_nx^*\right]. \tag{A5}$$

We therefore have a dimensionless inverse speed C_0K_r/ω and a dimensionless damping coefficient $-C_0K_i/\omega$. Meanwhile, the dimensionless frequency is a product: ω^*K_n. This means that for a fixed value of K_n, the Knudsen number is a simple scaling factor for the dimensionless frequency. Conversely, a fixed value of the dimensionless frequency is a simple scaling factor for the Knudsen number. Consequently, and for this particular configuration, one may absorb the factor K_n into ω^* and interpret the variation of their product as either Knudsen number or dimensionless frequency variations.

However, this description relies on the definition of the microscopic time τ as the time between molecule/molecule collisions. If this microscopic time is physically undefined, or becomes large, then Eq. (A5) and the interpretation that follows it become invalid because the product ω^*K_n is indeterminate. This is the case when the gas is confined between two surfaces so that collisions between molecules are no longer the most important mechanism of momentum transfer from one surface to the other, and instead the interactions of the molecules directly with the two surfaces (the source and receiver in the experiments) are.

In Greenspan's work, which has been followed by several authors, the nondimensionalization starts with a reference speed, denoted by $v_0=\omega/\beta_0$, which in our notation corresponds to ω/C_0, assuming an approximation of the dispersion at high pressure. Then the intermolecular collision mean time τ is determined assuming Maxwell molecules. The dimensionless sound speed and damping are given as they appear through Eq. (A5) while the inverse of the product ω^*K_n is referred to as "Reynold's number."

In any case, one can see easily from the expression C_0K_i/ω that for all theories predicting a finite value of the damping this dimensionless expression should give zero damping for ω tending to infinity. So, the expression, at first glance, is not even a well-indicated form to compare between different theoretical results in this field. A different analysis is therefore required.

Returning to Eq. (A1), for high Knudsen numbers, let us assume that the separation distance between the two surfaces, L, is the relevant microscopic parameter. With a C_0 that may be the thermal speed (or any other characteristic molecular speed), the average time spent traveling between the surfaces is now associated with τ.[8] As there are, on average, no intermolecular collisions in that period, we expect the wave propagation to become independent of the conventional Knudsen number beyond a certain limit. Equation (A1) is then written as

$$\phi(t,x)=\exp[i(\omega\tau t^*-L(K_r+iK_i)x^*)], \tag{A6}$$

which implies $\omega^*=\omega\tau$, $K^*=LK$, and the dimensionless sound speed and damping are given, respectively, by ω^*/K_r^* and $-K_i^*$, which are the expressions we defined in Eq. (33) (allowing for the constant coefficient $\sqrt{5/3}$). Moreover, this dimensionless phase speed and damping are independent of the dimensional frequency ω and so independent of ω_e.

Although our corrected dimensional analysis seems to work with the data in Ref. 5, further verifications with other experiments using reliable dimensionless parameters are necessary. It is also worth noting that the failure of Greenspan's analysis at high frequencies means that a high conventional Knudsen number does not necessarily mean a high frequency

and vice versa. In Fig. 7, ω is strictly speaking referring to a separation-distance-based Knudsen number, not the real dimensional frequency—as we have shown through Eq. (A6).

We have not compared our theoretical results with the more recent experimental data by Schotter.[8] This is because, while Schotter differentiated between two microscopic time scales, he defined the dimensionless parameters as in Greenspan's analysis, i.e., a dimensionless damping coefficient that depends on the frequency over the full regime. He reported different plots for different separation distances.

[1]D. A. Lockerby, J. M. Reese, and H. Struchtrup, "Switching criteria for hybrid rarefied gas flow solvers," Proc. R. Soc. London, Ser. A **465**, 1581 (2009).
[2]C. Cercignani, *Rarefied Gas Dynamics: From Basic Concepts to Actual Calculations* (Cambridge University Press, Cambridge, 2000).
[3]C. Cercignani, *Theory and Application of the Boltzman Equation* (Scottish Academy Press, Edinburgh and Elsevier, New York, 1975).
[4]M. Greenspan, "Propagation of sound in rarefied helium," J. Acoust. Soc. Am. **22**, 568 (1950).
[5]E. Meyer and G. Sessler, "Schallausbreitung in Gasen bei hohen Frequenzen und sehr niedrigen Drucken," Z. Phys. **149**, 15 (1957).
[6]D. Kahn and D. Mintzer, "Kinetic theory of sound propagation in rarefied gases," Phys. Fluids **8**, 1090 (1965).
[7]H. Struchtrup and M. Torrilhon, "Regularization of Grad's 13 moment equations: Derivation and linear analysis," Phys. Fluids **15**, 2668 (2003).
[8]R. Schotter, "Rarefied gas acoustics in the noble gases," Phys. Fluids **17**, 1163 (1974).
[9]J. K. Buckner and J. H. Ferziger, "Linearized boundary value problem for a gas and sound propagation," Phys. Fluids **9**, 2315 (1966).
[10]P. J. Dellar, "Macroscopic descriptions of rarefied gases from the elimination of fast variables," Phys. Fluids **19**, 107101 (2007).
[11]L. Sirovich and J. K. Thurber, "Propagation of forced sound waves in rarefied gas dynamics," J. Acoust. Soc. Am. **37**, 329 (1965).
[12]S. K. Loyalka and T. C. Cheng, "Sound-wave propagation in rarefied gas," Phys. Fluids **22**, 830 (1979).
[13]E. A. Spiegel and J.-L. Thiffeault, "Higher-order continuum approximation for rarefied gases," Phys. Fluids **15**, 3558 (2003).
[14]C. Cattaneo, "A form of heat conduction equation which eliminates the paradox of instantaneous propagation," Compt. Rend. **247**, 431 (1958).
[15]I. Muller, "Extended thermodynamics: The physics and mathematics of the hyperbolic equations of thermodynamics," International Series of Numerical Mathematics **141**, 733 (2001).
[16]N. Petrov and A. Szekeres, "New approach to the non-classical heat conduction," Journal of Theoretical and Applied Mechanics **38**, 61 (2008).
[17]Z. M. Zhang, *Nano Microscale Heat Transfer* (McGraw-Hill Professional, New York, 2007).
[18]S. K. Dadzie, J. M. Reese, and C. R. McInnes, "A continuum model of gas flows with localized density variations," Physica A **387**, 6079 (2008).
[19]H. Brenner, "Kinematics of volume transport," Physica A **349**, 11 (2005).
[20]H. Brenner, "Navier–Stokes revisited," Physica A **349**, 60 (2005).
[21]W. Marques, Jr., "Is Brenner's modification to the classical Navier–Stokes equations able to describe sound propagation in gases?" Chin. Phys. Lett. **25**, 1355 (2008).
[22]C. J. Greenshields and J. M. Reese, "The structure of shock waves as a test of Brenner's modifications to the Navier–Stokes equations," J. Fluid Mech. **580**, 407 (2007).
[23]M. Liu, "Comments on 'Weakly and strongly consistent formulations of irreversible processes'," Phys. Rev. Lett. **100**, 098901 (2008).
[24]G. Maidanik and H. L. Fox, "Comments on 'Propagation of forced sound waves in rarefied gasdynamics'," J. Acoust. Soc. Am. **38**, 477 (1965).
[25]M. Greenspan, "Attenuation of sound in rarefied helium," Phys. Rev. **75**, 197 (1949).
[26]W. Mandell and J. West, "On the temperature gradient in gases at various pressures," Proc. Phys. Soc. London **37**, 20 (1924).